Action of 2,3-butanedione monoxime on capacitance and electromotility of guinea-pig cochlear outer hair cells

Gregory I. Frolenkov, Fabio Mammano* and Bechara Kachar

*Section on Structural Cell Biology, Laboratory of Cellular Biology, NIDCD–NIH, Bethesda, MD, USA and *Laboratory of Biophysics and INFM Unit, International School for Advanced Studies, Trieste, Italy*

(Received 16 June 2000; accepted after revision 23 October 2000)

1. Whole-cell patch-clamp recordings were obtained from isolated cochlear outer hair cells (OHCs) while applying 2,3-butanedione monoxime (BDM) by pressure. BDM (5 mM) shifted the range of voltage sensitivity of membrane capacitance and cell length in the hyperpolarised direction by -49.6 ± 4.0 mV ($n = 12$; mean ± S.E.M.), without appreciable effects on membrane conductance. The shift was completely reversible and dose dependent, with a Hill coefficient of 1.8 ± 0.4 and a half-maximal dose of 3.0 ± 0.8 mM (values ± S.D).

2. The shift of the capacitance curve was also reproducible in cells whose natural turgor had been removed. BDM had no detectable effect on the capacitance of Deiters' cells, a non-sensory cell type of the organ of Corti.

3. The effect of BDM on membrane capacitance was faster than that of salicylate. At similar saturating concentrations (20 mM), the time constant of the capacitance changes was 1.8 ± 0.3 s ($n = 3$) for salicylate and 0.75 ± 0.06 s ($n = 3$) for BDM. The recovery periods were 13 ± 1 s and 1.7 ± 0.4 s, respectively (means ± S.E.M.).

4. The effect of BDM, a known inorganic phosphatase, was compared to the effects of okadaic acid, trifluoperazine and W-7, which are commonly used in studies of protein phosphorylation. Incubation of OHCs with okadaic acid (1 μM, 30–60 min) shifted the voltage sensitivity of the membrane capacitance in the hyperpolarised direction. Incubation with trifluoperazine (30 μM) and W-7 (150 μM) shifted it in the opposite, depolarised direction. BDM induced hyperpolarising shifts even in the presence of W-7.

5. Simultaneous measurement of membrane capacitance and intracellular free Ca^{2+} concentration ($[Ca^{2+}]_i$) showed that BDM action on OHC voltage-dependent capacitance and electromotility is not mediated by changes of $[Ca^{2+}]_i$.

6. Our results suggest that: (a) the effects of BDM are unrelated to its inorganic phosphatase properties, cell turgor conditions or Ca^{2+} release from intracellular stores; and (b) BDM may target directly the voltage sensor of the OHC membrane motor protein.

The membrane capacitance of OHCs is a function of transmembrane voltage (Ashmore, 1989). Although the detailed molecular mechanism remains to be established, this is thought to depend on aggregates of 'motor' proteins residing in the plasma membrane (reviewed in Frolenkov *et al.* 1998). Membrane motors have been postulated to possess a voltage sensor that generates fast asymmetric current transients at the onset and offset of voltage steps applied across the plasma membrane (Gale & Ashmore, 1997). The charge displacement associated with operation of the motors' voltage sensor imparts a characteristic bell-shaped dependence of membrane capacitance on transmembrane potential (Santos-Sacchi, 1991). Similar properties are displayed by gating charges in voltage-dependent ion channels (Armstrong, 1992), but the faster rate of charge translocation in OHCs suggests that the membrane motors are not modified ion channels (Géléoc *et al.* 1999). Rather than controlling ion flow, the voltage-driven conformation changes of the membrane motor proteins are thought to apply a stress to the plasma membrane changing the cell resting length, a phenomenon known as electromotility. Surface forces associated with local area changes in the plasma membrane (Kalinec *et al.* 1992) are presumably transferred to the underlying cortical cytoskeleton that contributes to the orientation of force output along the longitudinal axis of the cell (Holley *et al.* 1992; Kalinec *et al.* 1992; Tolomeo *et al.* 1996).

Only a few compounds, namely salicylate (Dieler *et al.* 1991; Tunstall *et al.* 1995), lanthanides (Santos-Sacchi, 1991; Kakehata & Santos-Sacchi, 1996) and sulfhydryl reagents (Kalinec & Kachar, 1993; Frolenkov *et al.* 1997) are presently known to block electromotility. Salicylate and lanthanides were additionally shown to eliminate the voltage-dependent fraction of the membrane capacitance (Santos-Sacchi, 1991; Tunstall *et al.* 1995; Kakehata & Santos-Sacchi, 1996). The operating range of the voltage-dependent capacitance is affected by a number of chemical reagents (Wu & Santos-Sacchi, 1998), none of which is likely to target selectively the putative membrane motors of the OHC.

In this paper we report the effects of an inorganic phosphatase, 2,3-butanedione monoxime (BDM), on OHC electromotility. BDM is capable of dephosphorylating acetylcholinesterases (Wilson & Ginsburg, 1955), as well as various smooth muscle proteins (Waurick *et al.* 1999). It also interferes with acto-myosin function through the myosin adenosine triphosphatase (ATPase) reaction shifting the equilibrium between two acto-myosin states towards the more weakly (pre-stroke) bound form (McKillop *et al.* 1994). In addition to its effect on the contractile apparatus, BDM promotes Ca^{2+} release from ryanodine-operated intracellular stores (Adams *et al.* 1998) and modulates ion (Lee *et al.* 1995; Ye & McArdle, 1995) and gating currents (Ferreira *et al.* 1997). We found that BDM shifts the operating range of the OHC voltage-dependent capacitance in an extremely rapid and reversible manner, more than any other chemical or physical manipulation reported so far.

METHODS

Cell preparation

Adult guinea-pigs (200–400 g) were killed by exposure to a rising concentration of carbon dioxide and decapitated, according to NIH guidelines for animal use. The temporal bones were removed from the skull and placed in a modified Leibowitz cell culture medium (L-15) containing (mM): NaCl (137), KCl (5.4), $CaCl_2$ (1.3), $MgCl_2$ (1.0), Na_2HPO_4 (1.0), KH_2PO_4 (0.44), $MgSO_4$ (0.81). The osmolarity was adjusted to 325 ± 2 mosmol l^{-1} with D-glucose and the pH was adjusted to 7.35 with NaOH. To isolate OHCs, the bulla was opened to expose the cochlea and the otic capsule was chipped away with a surgical blade starting from the base. Strips of the organ of Corti were dissected from the modiolus with a fine needle, transferred with a glass pipette to a 100 μl drop of medium containing 1 mg ml^{-1} of collagenase type IV (Life Technologies, Rockville, MD, USA), and kept there for 15–20 min. In some experiments, the strips were pre-incubated (30–60 min at 37°C) with drugs affecting protein phosphorylation: okadaic acid, trifluoperazine, and W-7 (Calbiochem, San Diego, CA, USA). As controls for these experiments, cells were maintained in standard medium for the same amount of time. After incubation, cells were dissociated by gentle reflux of the tissue through the needle of a Hamilton syringe (N. 705, 22 gauge) and allowed to settle on the slide for 5–10 min. OHCs were placed in a laminar flow bath (100 μl), in which solutions could be changed (about 5 ml h^{-1}) by means of a pressurised perfusion system (BPS-4; ALA Scientific Instruments, Westbury, NY, USA), and maintained at room temperature (22–24°C) throughout the experiments.

Patch-clamp recordings

OHCs were visualised under the microscope and the following morphological features were used to determine viability: uniform cylindrical shape, basal location of the nucleus, membrane birefringence and intact stereocilia. In most experiments, patch-clamp pipettes were filled with a CsCl-based intracellular solution containing (mM): CsCl (140), $MgCl_2$ (2.0), EGTA (5.0), Hepes (5), adjusted to pH 7.2 with CsOH and brought to 325 mosmol l^{-1} with D-glucose. In some experiments involving the pressure application of BDM and sodium salicylate, the intracellular solution contained (mM): KCl (144), $MgCl_2$ (2.0), EGTA (0.5), Na_2HPO_4 (8.0), NaH_2PO_4 (2.0), Mg-ATP (2.0), Na-GTP (0.2), adjusted to pH 7.2 with KOH and brought to 325 mosmol l^{-1} with D-glucose. For Ca^{2+} imaging experiments, this solution was supplemented with 0.1 mM Oregon Green 488 BAPTA-1 (Molecular Probes).

Patch-clamp recordings were performed using an Axopatch-1D amplifier (Axon Instruments). Pipettes for conventional whole-cell recordings were formed on a programmable puller (P87, Sutter Instruments) from 1.0 mm o.d. borosilicate glass (no. 30-30-0, FHC, Bowdoinham, ME, USA). Current and voltage were sampled at 100 kHz using a standard laboratory interface (Digidata 1200A, Axon Instruments) controlled by pCLAMP 7.0 software (Axon Instruments). The uncompensated pipette resistance was typically 3–5 MΩ when measured in the bath and the access resistance did not exceed 15 MΩ under whole-cell patch-clamp conditions. Potentials were corrected off-line for the error due to the access resistance. Junction potentials were −4.2 mV for the KCl-based solution and −4.9 mV for the CsCl-based solution, as computed by the pCLAMP 7.0 software using the given solution composition. These values were very similar and rather small, and therefore no correction was applied to the data for liquid junction potentials.

Drug delivery

A puff pipette, prepared similarly to the patch pipette, was filled with BDM, sodium salicylate or ionomycin (Sigma), dissolved in the extracellular solution. It was placed near the basolateral wall of the OHC and pressure (10–15 kPa) was applied to its back by a pneumatic injection system (PLI-100, Medical Systems Corp., Greenvale, NY, USA) gated under software control. Typical drug delivery time was $\leqslant$ 30 ms, as determined by positioning the patch pipette in front of the puff pipette and monitoring the change in junction potential.

Capacitance measurement

Measurements of membrane capacitance were derived from those of asymmetric currents evoked by pre-stepping the cell potential to large hyperpolarised values (V_{pre}), around −160 mV, for about 1 ms from a holding potential (V_h) of −60 mV, followed by depolarising steps of variable amplitude and 2–3 ms duration. The potential was then returned to V_{pre} for 2–3 ms before resetting it to V_h, preparing the cell for the next step (Fig. 1, right inset). Charge movement Q was estimated by time integration of the asymmetric currents at the step offset, when the cell was temporarily returned to V_{pre}, i.e. under constant driving force conditions. As the time constant of the patch-clamp recording was in the range 0.1–0.3 ms, more than 99% of the current had settled within 2 ms. Leakage currents were estimated and subtracted off-line by assuming that asymmetric currents had completely decayed at the end of the eliciting pulse. This procedure was found to introduce less noise than the standard $P/4$ technique (Armstrong & Bezanilla, 1977). In most cases, ionic currents were not activated appreciably during the brief voltage commands applied.

Alternatively, measurements of membrane capacitance were performed using the 'membrane test' feature of the pCLAMP 7.0 acquisition software, which continuously delivered a test square wave

of period $T = 4$ ms to the cell, through the patch-clamp amplifier. This produced transient currents that decayed exponentially with a (voltage-dependent) time constant τ. The software was designed for the simultaneous on-line measurement of τ, the total resistance, R_t, recorded by the amplifier, and the electrical charge delivered to the membrane (membrane capacitance), C_m. Unfortunately the pCLAMP software accurately estimates parameters R_m (cell membrane resistance), R_a (pipette access resistance) and C_m only if $R_m \gg R_a$, a condition which was not always met. To circumvent this problem, we reversed the pCLAMP algorithm off-line to recover the original values for the time integral of the transient current, Q and R_t. We then re-computed R_m, R_a and C_m according to the equations shown below. The voltage step V elicited a whole-cell current:

$$i = \frac{V}{R_m + R_a}\left(1 + \frac{R_m}{R_a}\exp(-t/\tau)\right),$$

$$\text{where } \tau = \frac{R_m R_a}{R_m + R_a} C_m. \quad (1)$$

The charge delivered to the equivalent circuit by the transient current:

$$Q = \int_0^{T/2} \frac{V R_m}{(R_m + R_a)R_a}\exp(-t/\tau)\mathrm{d}t$$

$$= VC_m\left(\frac{R_m}{R_m + R_a}\right)^2 [1 - \exp(-T/2\tau)], \quad (2)$$

and the total resistance is:

$$R_t = R_m + R_a. \quad (3)$$

Solving simultaneously eqns (1), (2) and (3) yields:

$$R_a = R_t \Big/ \left(1 + \frac{QR_t}{\tau V[1 - \exp(-T/2\tau)]}\right);$$

$$R_m = R_t - R_a;$$

$$C_m = \frac{Q}{V}\left(\frac{R_t}{R_m}\right)^2 \frac{1}{1 - \exp(-T/2\tau)}. \quad (4)$$

The patch parameters were continuously monitored, at a resolution of 25 Hz, by averaging the responses to 10 positive and 10 negative consecutive test steps. The series resistance and linear capacitance compensation circuitry of the patch-clamp amplifier was not used. Instead, to obtain the voltage dependence of C_m we applied triangular voltage ramps, swinging the cell potential from $V_h = -100$ mV to $V_h = +160$ mV in 6 s (Fig. 1, left inset). Before the C_m calculation, the values of total resistance $R_{t,0}$, estimated by pCLAMP 7.0, were corrected for the slope of the ramp as follows:

$$R_t = V/[(V/R_{t,0}) - \Delta I], \quad (5)$$

where ΔI is the increment of the whole-cell current produced by voltage ramp in $T/2 = 2$ ms.

To test the accuracy of the C_m determination, we performed measurements of C_m on a model electronic circuit in which we varied R_m from 500 to 5 MΩ keeping $R_a = 10$ MΩ constant and C_m equal to one of three values: 10, 20 or 30 pF. The values of C_m, calculated according to the above procedure, differed from their nominal values by no more than 2 pF, provided that $R_m/R_t > 0.6$. Under these conditions, the estimate of C_m did not vary significantly when the voltage was commanded to follow a ramp. Large errors in the C_m estimate occurred at $R_m/R_t < 0.6$ because the amplitude of the exponentially decaying transient current was less than the steady-state current response to the test step. The pCLAMP algorithm was then unable to 'lock' the exponential decay and to calculate its time constant. Therefore, all data points obtained when $R_m/R_t \leqslant 0.6$ have been excluded from the analysis. Measurements of the membrane capacitance during test ramps were fitted with:

$$C_m(V) = C_0 + C_{\text{non-lin}}(V) = C_0 + 4C_{\max}\left(\frac{\exp(-(V - V_p)/W)}{[1 + \exp(-(V - V_p)/W)]^2}\right), \quad (6)$$

which is the derivative of a Boltzmann function. C_0 is the linear (voltage-independent) capacitance, $C_{\text{non-lin}}$ is the non-linear (voltage-dependent) capacitance, $C_{\max}$ is the maximum voltage-dependent capacitance, V_p is the potential at the peak of $C_m(V)$ or mid-point potential and $W = k_B T/ze$ is a constant that is a measure of the sensitivity of the non-linear charge displacement to potential. W is expressed in terms of a charge of valency z moving from the inner to the outer aspect of the plasma membrane. k_B is Boltzmann's constant, T is absolute temperature and e is the electron's charge.

The voltage-independent fraction of the membrane capacitance scales linearly with the overall surface area of the cell, whereas its voltage-dependent fraction is proportional to the area of the lateral membrane surface, where the putative motor elements are located (Huang & Santos-Sacchi, 1993). Therefore, in order to compare the data obtained from different cells, the voltage-dependent

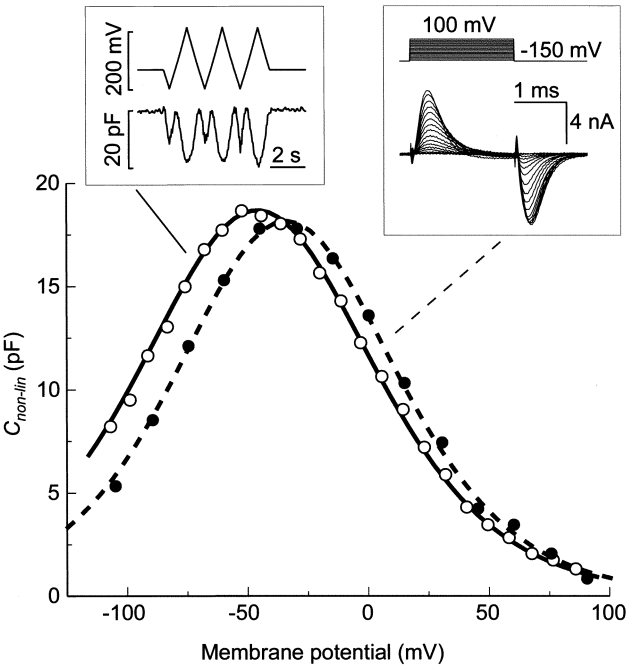

Figure 1. Measurements of voltage-dependent capacitance of isolated outer hair cell

○, capacitance values derived by the membrane test method during the application of a ramp protocol (left inset); ●, values derived by applying the step protocol (right inset) to the same cell. Data were fitted to the derivative of a Boltzmann function (continuous and dashed lines, respectively). Parameters of the fits: $C_{\max} = 18.7 \pm 0.2$ pF, $V_p = -45.8 \pm 0.3$ mV, $W = 32.2 \pm 0.3$ mV (membrane test method); $C_{\max} = 18.2 \pm 0.3$ pF, $V_p = -33.7 \pm 0.6$ mV, $W = 31.5 \pm 0.5$ mV (step protocol). The patch pipette was filled with the CsCl-based intracellular solution (see Methods).

capacitance was divided by the area of the lateral plasma membrane as follows:

$$\chi_m(V) = (C_m(V) - C_0)/[(C_0 - C_{ap} - C_{bas})/\chi_{lb}], \quad (7)$$

where $\chi_m(V)$ is the specific voltage-dependent capacitance of the lateral plasma membrane (in μF cm^{-2}). C_{ap} (4.38 pF) and C_{bas} (1.85 pF) are the capacitances of the apical and basal parts of OHC, devoid of motor proteins (Huang & Santos-Sacchi, 1993). Therefore the difference formula $C_0 - C_{ap} - C_{bas}$ gives the linear voltage-independent capacitance of the lateral plasma membrane. χ_{lb} (1 μF cm^{-2}) is the specific capacitance of the lipid bilayer.

The two methods of capacitance measurement described above produced similar results (Fig. 1). In general, however, the capacitance curve obtained by the step method was shifted in the depolarised direction. This is a consequence of pre-stepping the holding potential to highly hyperpolarised values. Pre-pulse delivery is known to affect the voltage at peak capacitance: depolarisation shifts V_p in the hyperpolarising direction, and hyperpolarisation does the opposite (Santos-Sacchi *et al.* 1998). All experiments using drug application by pressure were performed using the more accurate membrane test method. However, to compute the statistical results shown in Fig. 3*B* the faster step method was adopted. Data obtained with different methods were never combined.

Motility measurements

Motility measurements were performed as described in Frolenkov *et al.* (1997). Briefly, OHC movements were recorded with a video camera interfacing with an inverted microscope equipped with differential interference contrast optics to an optical disk recorder

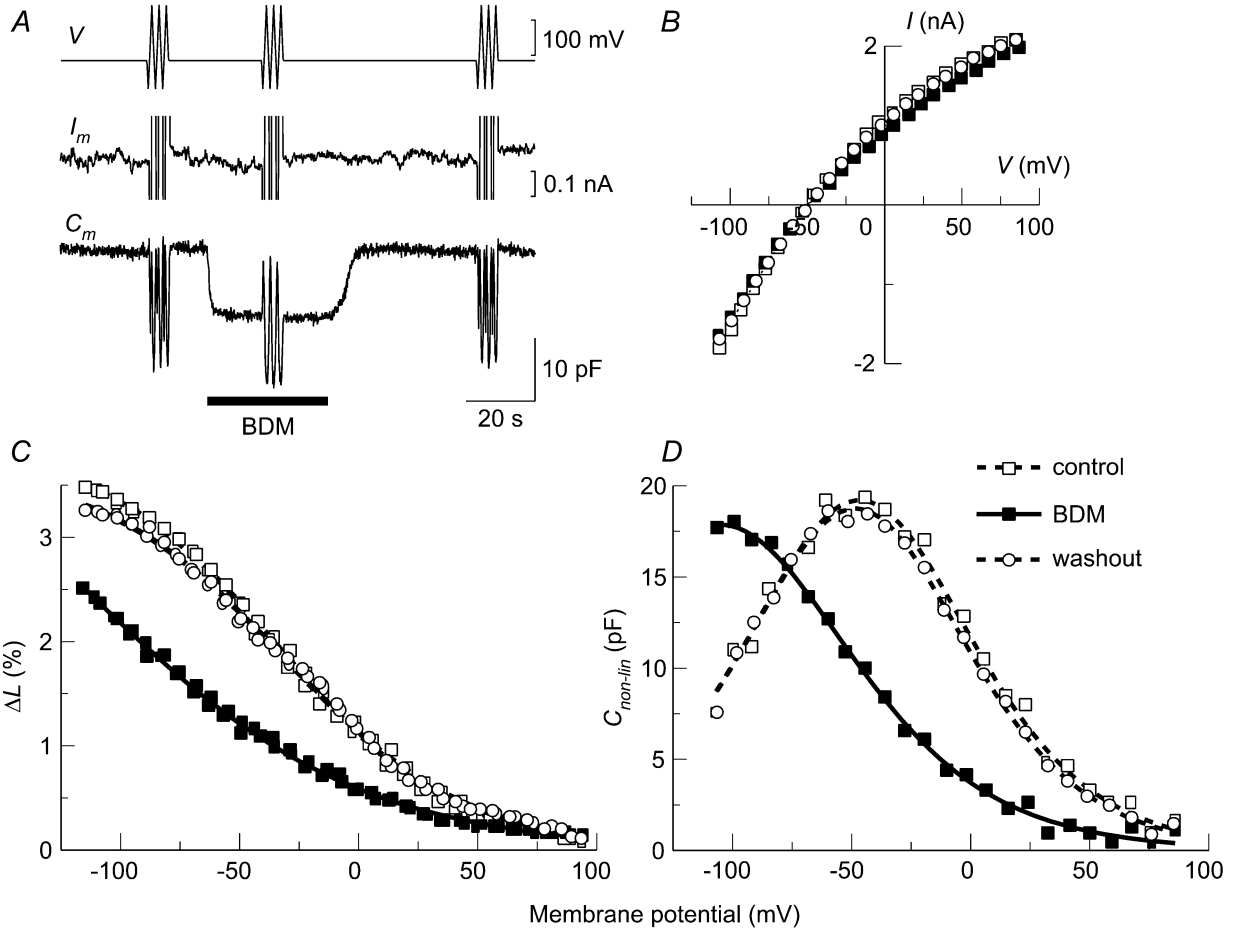

Figure 2. Effect of BDM on the voltage-dependent capacitance and electromotile responses

A, voltage stimuli applied by the patch-clamp amplifier (V), whole cell current (I_m) and membrane capacitance (C_m) responses. Holding potential (V_h) = −50 mV. I_m is clipped during voltage ramps to show the absence of the BDM effect on the baseline current. Note rapid and reversible drop of C_m during BDM application (20 mM, 35 s; filled bar). *B–D*, current–voltage relationships (*B*), percentage length change (*C*) and voltage-dependent fraction of the capacitance (*D*), measured before (□), during (■) and after (○) the application of BDM. Parameters of the fits for the electromotility data in (*C*): $L_{max}/L_0 = 3.9 \pm 0.1$ %, $V_p = -33 \pm 1$ mV, $W = 37 \pm 1$ mV (control); $L_{max}/L_0 = 4.9 \pm 0.5$%, $V_p = -114 \pm 11$ mV, $W = 57 \pm 4$ mV (BDM); $L_{max}/L_0 = 3.7 \pm 0.1$ %, $V_p = -31 \pm 1$ mV, $W = 38 \pm 1$ mV (washout). Parameters of the fits for the capacitance data in (*D*): $C_{max} = 19.2 \pm 0.3$ pF, $V_p = -46.7 \pm 0.9$ mV, $W = 31.8 \pm 0.7$ mV (control); $C_{max} = 17.9 \pm 0.4$ pF, $V_p = -105 \pm 4$ mV, $W = 37 \pm 2$ mV (BDM); $C_{max} = 18.7 \pm 0.3$ pF, $V_p = -48.4 \pm 0.8$ mV, $W = 31.2 \pm 0.4$ mV (washout). Data in *A–D* are from the same cell. The patch pipette was filled with the KCl-based intracellular solution.

(Panasonic TQ-3031F). Digitised images were analysed off-line with the image-processing system Image 1 (Universal Imaging, West Chester, PA, USA). For movement quantification, a measuring rectangle ranging in length from 5 to 20 μm and composed of 3–15 rows of pixels was positioned across the moving edge of the cell. The average intensity profile across the edge of the cell was calculated and the number of points in the profile was increased 10 times by cubic spline interpolation. Movement of the cell edge was calculated from the frame-by-frame shift (computed by a least-squares procedure) in the interpolated intensity profiles. The sensitivity of the measurement was ~0.02 μm, as previously determined (Frolenkov *et al.* 1997). Data obtained in this way were fitted by a scaled Boltzmann function:

$$\frac{\Delta L}{L_0}(V) = \frac{\Delta L_{max}}{L_0}\left(1 - \frac{1}{1+\exp(-(V-V_p)/W)}\right). \quad (8)$$

Here L_0 is the length of the cell at the holding potential V_h, whereas ΔL_{max} is the maximum voltage-dependent length change. V_p and W have the same meaning as in the expression for the voltage-dependent capacitance.

Ca^{2+} fluorescence imaging

Light from a 175 W stabilised xenon arc source (Lambda DG-4, Sutter Instruments) was coupled via a liquid light guide to the epifluorescence section of an Axiomat microscope (Carl Zeiss), which was equipped with an Omega Optical XF100 filter-block optimised for the Ca^{2+}-selective dye Oregon Green 488 BAPTA-1. The illumination intensity was attenuated with a neutral density filter to avoid phototoxicity by reducing dye photo-bleaching rates to $\leqslant 0.1\,\% \, s^{-1}$. Fluorescence images were formed on a scientific grade cooled CCD sensor (Micromax 1300Y, Princeton Instruments) using an oil-immersion objective (×100, NA 1.40; PlanApo, Carl Zeiss). The sensor's output was binned 3 × 3 and digitised at 12 bits per pixel to produce 400 × 330 pixel images that were recorded to a host PC controlled by the Axon Imaging Workbench software (Axon Instruments) and analysed off-line. For each image pixel, fluorescence signals were computed as ratios $\Delta F/F = [F(t) - F(0)]/F(0)$, where t is time, $F(t)$ is fluorescence following a stimulus that causes Ca^{2+} elevation within the cell, and $F(0)$ is pre-stimulus fluorescence computed by averaging 10–20 images. Both $F(t)$ and $F(0)$ were corrected for mean background fluorescence computed from a 20 × 20 pixel rectangle devoid of obvious cellular structures.

All values are given as means ± S.E.M. unless otherwise stated. Statistical significance was estimated using Student's t test at the $P \leqslant 0.05$ level. Curves generated by text equations were fitted to data by a Levenberg-Marquardt algorithm using Origin 6.0 software (Microcal Software, Northampton, MA, USA). This software also estimated the standard errors of fitting parameters.

RESULTS

Effect of BDM on the voltage-dependent capacitance and length change

Pressure application of BDM to isolated OHCs had no effect on the whole-cell current at holding potentials, V_h, between −70 mV and −50 mV. However, BDM induced rapid and substantial drops of the membrane capacitance at V_h (Fig. 2*A*). The latency of this effect did not exceed 30 ms, which corresponded to the typical drug delivery time in the present experiments (see Methods). Following the application of BDM, the current–voltage relationship, determined by subjecting the membrane potential to a

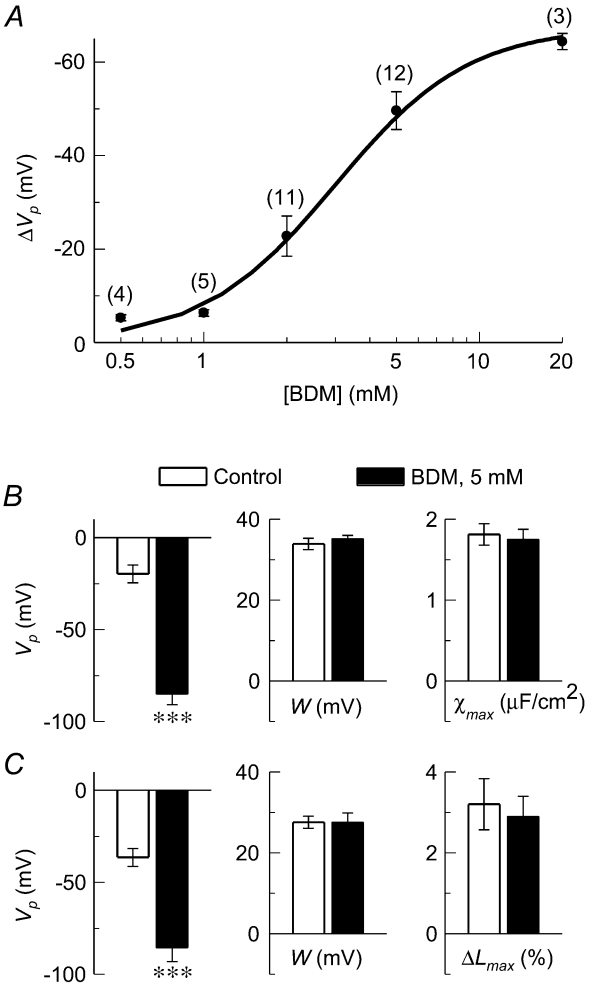

Figure 3. Pooled data showing BDM effects on capacitance and motility

A, dose–response curve showing the change in the mid-point (V_p) of the voltage dependence of the membrane capacitance *vs.* BDM concentration. Each point is the mean ± S.E.M. of the indicated number of cells. Continuous line through data is a non-linear fit obtained from the generalised logistic function $y = [BDM]^h/([BDM]^h + K_A{}^h)$, where the exponent h is the Hill coefficient and K_A is the half-saturating concentration of BDM. Parameters of the fit: $h = 1.8 \pm 0.4$, $K_A = 3.0 \pm 0.8$ mM. *B*, Boltzmann parameters describing the dependence of cell capacitance on membrane potential in the control cell group (open bars; $n = 7$) and in cells treated with 5 mM BDM (filled bars; $n = 8$): V_p, mid-point potential; W, voltage sensitivity; and χ_{max}, maximum voltage-dependent capacitance per square centimetre of lateral plasma membrane. *C*, Boltzmann parameters of the electromotility responses measured in the same groups: V_p and W as above; ΔL_{max}, maximum motile response as a percentage of the length of the cell at holding potential. *** $P < 0.001$. Data were obtained using the CsCl-based intracellular solution.

voltage ramp from −110 mV to 90 mV in 6 s, showed minor and reversible changes only at voltages above −20 mV (Fig. 2*B*). Instead, the voltage dependence of the cell length (Fig. 2*C*) and membrane capacitance (Fig. 2*D*) shifted in the hyperpolarised direction without any visible change in cell morphology. The shift was completely reversible and dose dependent (Fig. 3*A*), with a Hill coefficient of 1.8 ± 0.4 and a half-maximal dose of 3.0 ± 0.8 mM. The main parameter affected by BDM was the mid-point potential, V_p, of the voltage-dependent capacitance and length change (Fig. 3*B* and *C*). The membrane capacitance of Deiters' cells, a non-sensory cell type of the organ of Corti, was unaffected by the application of BDM (0.2–20 mM; data not shown).

Effect of intracellular pressure removal on the capacitance response to BDM

Cell turgor (intracellular pressure) is an important factor in the control of OHC electromotility (Shehata *et al.* 1991; Chertoff & Brownell, 1994) and voltage-dependent capacitance (Iwasa, 1993; Kakehata & Santos-Sacchi, 1995). To eliminate the potentially confounding effects of turgor changes, we tested the effect of BDM on OHCs whose turgor had been reduced by applying negative pressure to the back of the patch pipette. The change in the mid-point potential, $\Delta V_p = -47.5 \pm 5.2$ mV ($n = 5$),

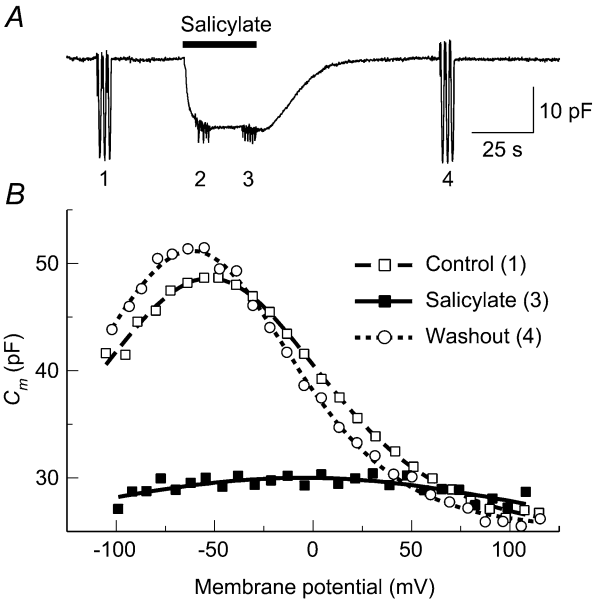

Figure 4. Effect of salicylate on the voltage-dependent capacitance.

A, membrane capacitance measured before, during (filled bar) and after the pressure application of sodium salicylate (20 mM). *B*, voltage dependence of the OHC capacitance derived from the responses to the voltage ramps (numbered from 1 to 4 in *A*) before (□), during (■) and after (○) the application of salicylate. Parameters of the fits: $C_0 = 25.0 \pm 0.3$ pF, $C_{max} = 23.6 \pm 0.3$ pF, $V_p = -52.7 \pm 0.7$ mV, $W = 39.3 \pm 0.9$ mV (control); $C_0 = 21 \pm 24$ pF, $C_{max} = 9 \pm 24$ pF, $V_p = -5 \pm 6$ mV, $W = 96 \pm 158$ mV (salicylate); $C_0 = 25.3 \pm 0.3$ pF, $C_{max} = 25.9 \pm 0.3$ pF, $V_p = -61.5 \pm 0.7$ mV, $W = 34.7 \pm 0.8$ mV (washout). The patch pipette was filled with the KCl-based intracellular solution. Compare Fig. 2*A* and *D*.

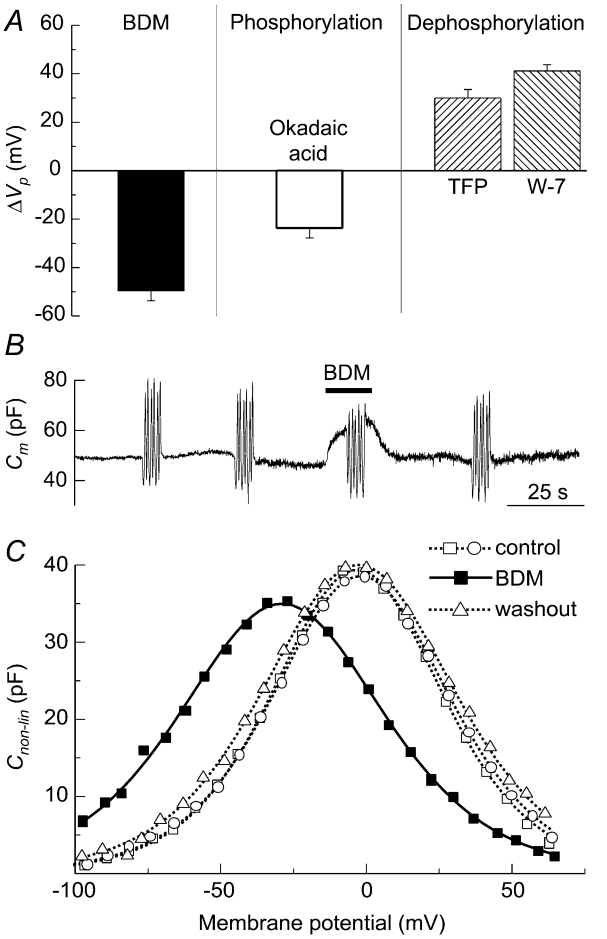

Figure 5. Comparison of the effects of BDM and protein phosphorylation on the voltage-dependent capacitance

A, changes in the mid-point potential (V_p; means ± S.E.M.) following the application of BDM (5 mM, $n = 12$), okadaic acid (1 μM, $n = 6$, a phosphorylation promoter), and two inhibitors of Ca^{2+}–calmodulin-dependent protein phosphorylation, trifluoperazine (TFP; 30 μM, $n = 5$) and W-7 (150 μM, $n = 7$). All changes were significant ($P < 0.001$). *B*, OHC capacitance responses to the application of BDM (5 mM, filled bar) in the presence of W-7 (150 μM). *C*, voltage dependence of the membrane capacitance, derived from the raw ramp responses shown in *B* (control, □ and ○; BDM, ■; washout, △). Parameters of the fits: $C_{max} = 39.3 \pm 0.4$ pF and 38.4 ± 0.5 pF, $V_p = -3.2 \pm 0.6$ mV and -1.9 ± 0.7 mV, $W = 19.4 \pm 0.4$ mV and 20.2 ± 0.4 mV (control); $C_{max} = 34.9 \pm 0.3$ pF, $V_p = -29.1 \pm 0.5$ mV, $W = 23.2 \pm 0.3$ mV (BDM); $C_{max} = 39.9 \pm 0.3$ pF, $V_p = -2.7 \pm 0.3$ mV, $W = 21.9 \pm 0.2$ mV (washout). Data were obtained using the KCl-based intracellular solution.

produced by BDM (5 mM) in these collapsed cells was statistically significant ($P < 0.001$) and was similar to that of the control group (Fig. 3*B*), indicating that BDM can affect the voltage dependence of the capacitance also in the absence of turgor changes.

Comparing the effects of BDM and salicylate

Acetylsalicylic acid has a number of reversible effects on the auditory system and, when applied to OHCs *in vitro*, it produces a remarkable reduction of electromotility and associated voltage-dependent capacitance (Tunstall *et al.* 1995). The time course of the sodium salicylate effect on the membrane capacitance is shown in Fig. 4*A*, for comparison with that of BDM (Fig. 2*A*). At equally saturating concentrations (20 mM), the onset time constant of the capacitance changes obtained by a single exponential fit was 1.8 ± 0.3 s ($n = 3$) for salicylate and 0.75 ± 0.06 s ($n = 3$) for BDM. The difference is statistically significant ($P < 0.05$). The recovery period following the application of salicylate (13 ± 1 s) was significantly longer ($P < 0.0001$) than the recovery period following the application of BDM (1.7 ± 0.4 s). Salicylate reduced the peak value of the capacitance by more than 90 % (Fig. 4*B*) without major shifts in V_p, indicating that the mechanisms of action of the two drugs are different (compare Fig. 2*D*).

Comparing the effects of BDM and protein phosphorylation

As an inorganic phosphatase, BDM has been used to modify the phosphorylation state of many cellular proteins (Eisfeld *et al.* 1997). In Fig. 5*A* the effect of BDM on the voltage-dependent capacitance of OHCs is compared to that of other drugs commonly used in studies of protein phosphorylation. Following incubation in okadaic acid (1 μM, 30–60 min at 37°C), a powerful inhibitor of the protein phosphates-1 and -2A that promote phosphorylation of a wide range of proteins *in vivo* (Haystead *et al.* 1989), V_p shifted in the hyperpolarised direction. Incubation for 30–60 min with the specific calmodulin inhibitors trifluoperazine (30 μM) and W-7 (150 μM) (Johnson & Wittenauer, 1983) shifted V_p in the opposite, depolarised direction. The effects of these reagents did not depend on the intracellular pressure and were reproducible in both the cells with normal turgor and the cells collapsed by a gentle suction through the patch pipette. Furthermore, the experiment in Fig. 5*B* and *C* shows that the ability of BDM to shift V_p in the hyperpolarised direction was unaffected by the blockade of Ca^{2+}–calmodulin-dependent phosphorylation obtained with 150 μM W-7, a saturating concentration (Hidaka *et al.* 1981; Itoh & Hidaka, 1984). Since the voltage dependence of C_m was significantly shifted in the depolarising direction in the presence of W-7, BDM produced a transient increase of C_m baseline (Fig. 5*B*) in contrast to the typical decrease of C_m observed in control conditions (Fig. 2*A*). However, the shifts of V_p induced by 5 mM BDM in the presence of W-7 ($\Delta V_p = -29 \pm 2$ mV, $n = 3$)

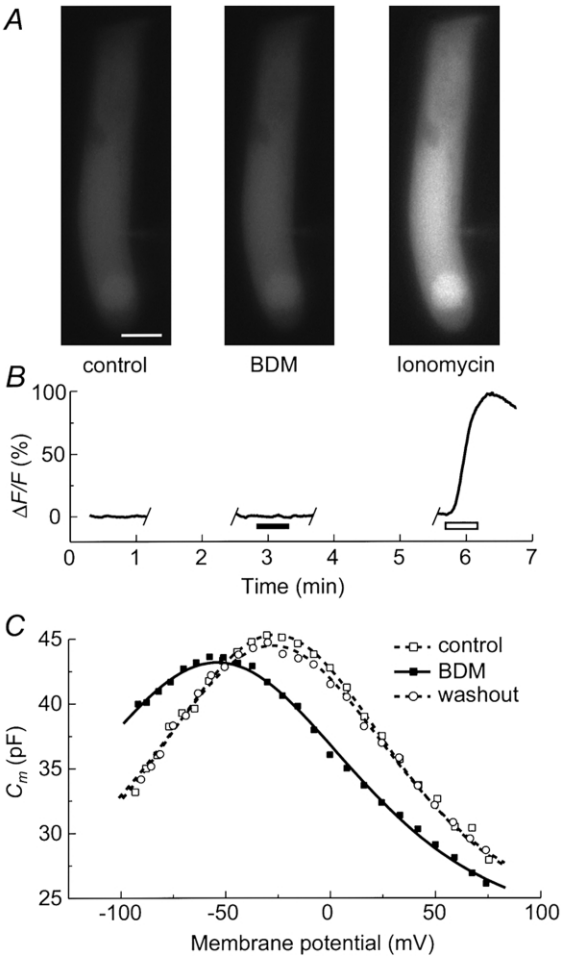

Figure 6. The effect of BDM is not mediated by an increase of intracellular free Ca^{2+} concentration

A, fluorescence images of an OHC loaded with 100 μM Oregon Green 488 BAPTA-1 through the patch pipette before (left), immediately after the application of BDM (5 mM; middle), and after the subsequent application of ionomycin (10 μM; right). Scale bar: 10 μm. *B*, percentage fluorescence responses, relative to the pre-stimulus condition, of the cell in *A* to the consecutive applications of BDM (middle, filled bar) and ionomycin (right, open bar). $V_h = -60$ mV. The fluorescence intensity trace was obtained by averaging pixel values over the whole cell body. *C*, voltage dependence of the membrane capacitance of the same OHC measured before (□), during (■), and after (○) the application of BDM shown in *A* and *B*. Parameters of the fits: $C_0 = 24 \pm 1$ pF, $C_{max} = 21.4 \pm 0.9$ pF, $V_p = -26.2 \pm 0.7$ mV, $W = 37 \pm 2$ mV (control); $C_0 = 23.6 \pm 0.5$ pF, $C_{max} = 19.8 \pm 0.4$ pF, $V_p = -54.0 \pm 0.7$ mV, $W = 40 \pm 1$ mV (BDM); $C_0 = 24.3 \pm 0.9$ pF, $C_{max} = 20.1 \pm 0.8$ pF, $V_p = -27.6 \pm 0.7$ mV, $W = 36 \pm 2$ mV (washout). The patch pipette was filled with the KCl-based intracellular solution.

and in the control conditions (Fig. 5*C*) were comparable. These results suggest that the effect of BDM on the OHC capacitance is not related to its activity as an inorganic phosphatase.

Effect of BDM on the intracellular Ca^{2+} concentration

To determine whether intracellular free Ca^{2+} plays any role in the action of BDM on membrane capacitance, we used fluorescence microfluorimetry and monitored cytoplasmic Ca^{2+} levels in OHCs loaded with Oregon Green 488 BAPTA-1 (100 μM), a single wave-length fluorescent probe highly selective for this divalent cation. As shown in Fig. 6*A* and *B*, no fluorescence change was detected either during or following the application of BDM (5 μM, $n = 5$), although sizeable capacitance changes were evoked (Fig. 6*C*). The Ca^{2+} ionophore ionomycin was subsequently applied to the cell through a second puff pipette. This drug is known to induce a generalised, transient increase of $[Ca^{2+}]_i$ by making the plasma membrane, as well as the membranes of intracellular Ca^{2+} stores, permeable to Ca^{2+}. As expected, ionomycin elevated intracellular Ca^{2+} ($n = 3$) even after the application of BDM (Fig. 6*A*, right; Fig. 6*B*, right), indicating that the absence of Ca^{2+} responses to BDM was not a consequence of a high basal level of the $[Ca^{2+}]_i$ or low sensitivity of the measuring technique. In fact, a second application of ionomycin produced a distinguishable, albeit small, increase of $[Ca^{2+}]_i$ suggesting that the basal level of $[Ca^{2+}]_i$ in the OHCs was well below the saturating level for the Oregon Green (300–400 nM).

DISCUSSION

BDM is a clinically used drug that is known to exert multiple and complex effects on cell physiology (see Introduction). We found that it rapidly and reversibly affects the operating range of the voltage-dependent capacitance and length changes of OHCs, shifting both of them in the hyperpolarised direction more than any other drug or manipulation (Kakehata & Santos-Sacchi, 1995; Santos-Sacchi *et al.* 1998; Santos-Sacchi & Huang, 1998) reported so far. The action of BDM on the OHC capacitance and electromotility is entirely reversible and extremely rapid both at the onset and at the offset of the drug application (Fig. 2).

The operating range of the voltage-dependent capacitance and length change has been reported to shift in the hyperpolarised direction following the decrease in intracellular pressure (cell turgor), which alters the tension in the plasma membrane (Iwasa, 1993; Gale & Ashmore, 1994; Kakehata & Santos-Sacchi, 1995). To eliminate these potentially confounding effects, we applied BDM to cells that had been collapsed by applying gentle suction through the patch pipette. The shifts of the operating range of the voltage-dependent capacitance observed under these conditions were similar to the controls, indicating that BDM action is unlikely to be mediated by turgor changes altering membrane tension.

Protein dephosphorylation and voltage-dependent capacitance

As an inorganic phosphatase, BDM may dephosphorylate a number of different proteins (Green & Saville, 1956; Coulombe *et al.* 1990). In our experiments BDM shifted the operating range of OHC electromotility and voltage-dependent capacitance in the hyperpolarised direction. In contrast, drugs that promote protein dephosphorylation, W-7 and trifluoperazine (Johnson & Wittenauer, 1983), induced depolarising shifts. Hyperpolarising shifts were observed after exposure to okadaic acid, which promotes the phosphorylation of a wide range of proteins *in vivo* (Haystead *et al.* 1989). In fact, when BDM was applied to cells incubated and bathed in W-7, its effects were remarkably similar to those produced under control conditions. We conclude that the effects of BDM on OHCs cannot be explained by its action as a phosphatase.

Role of intracellular Ca^{2+}

A system of flattened, membrane-bound intracellular compartments, the *subsurface cisternae*, is found in the closest proximity to the electromotility machinery, at nanometre distances below the cortical lattice (Holley *et al.* 1992). The preferential distribution of Ca^{2+}-ATPase near the innermost layer of the cisternae, in strict apposition to linearly arranged mitochondria (Schulte, 1993; Ikeda & Takasaka, 1993), supports a role for these structures as intracellular stores of Ca^{2+}. The increase of free Ca^{2+} concentration has been shown to induce circumferential contraction and longitudinal elongation of the OHC (Dulon *et al.* 1990). Inhibition of these effects by calmodulin antagonists (Dulon *et al.* 1990) and antagonists of calmodulin-dependent kinases (Puschner & Schacht, 1997; Coling *et al.* 1998) suggests the involvement of Ca^{2+}–calmodulin-dependent protein phosphorylation. BDM has been reported to promote the release of Ca^{2+} from the sarcoplasmic reticulum of skeletal and cardiac muscle (Tripathy *et al.* 1999) by modulating ryanodine receptors (Adams *et al.* 1998). However, fluorescence imaging experiments like the one shown in Fig. 6 indicate that the action of BDM on OHC membrane capacitance does not appear to involve mobilisation of intracellular Ca^{2+}. We still cannot rule out the possibility that localised sub-membrane changes of $[Ca^{2+}]_i$ occur and pass undetected by our fluorescence imaging. On the other hand, the fast recovery of the capacitance after BDM and the inability of the ionomycin-induced increase of $[Ca^{2+}]_i$ to modulate the capacitance (Frolenkov *et al.* 2000), argue against the possibility that the BDM effect on OHC is mediated by $[Ca^{2+}]_i$.

We did not observe any morphological changes in OHCs either during or after the application of BDM, suggesting that it does not affect (directly or indirectly) the cytoskeleton of the OHC. Therefore, it is unlikely that

BDM action is mediated by changes in membrane tension associated with modification of the OHC cytoskeletal structure, such as those produced by BDM in muscle cells (McKillop *et al.* 1994).

Mechanism of action of BDM

It has been proposed that BDM exerts its inhibitory action on K_{ATP} channels (Smith *et al.* 1994) as well as L-type Ca^{2+} channels (Eisfeld *et al.* 1997; Allen *et al.* 1998) by mechanisms unrelated to protein dephosphorylation. Consistent with these findings, our results indicate that the effects of BDM on OHCs are not related to its inorganic phosphatase properties. Instead, the time course, reversibility, lack of dependence on intracellular Ca^{2+}, together with the magnitude and the direction of the shift of the voltage-dependent capacitance induced by BDM suggest that BDM may directly target the voltage sensor of the OHC putative membrane motors. Interestingly, the gating charge movement of the L-type Ca^{2+} channel has been shown to be reduced after the application of BDM (Ferreira *et al.* 1997). Thus, the unique characteristics of BDM might be useful to the study of the mechanisms by which the recently proposed candidates for OHC motor protein, the sugar transporter GLUT5 (Géléoc *et al.* 1999) and a protein called 'prestin' (Zheng *et al.* 2000), could act as sensors of transmembrane potential.

Finally, BDM is used clinically for its protective actions on human myocardial force production (Perreault *et al.* 1992). Another class of drugs widely used in clinical practice, salicylates, are known to target OHC electromotility (Tunstall *et al.* 1995) and have ototoxic side effects (Stypulkowski, 1990). The distinct and powerful action of BDM on OHC electromotility indicates that this compound should be evaluated for its potential effects on hearing.

Adams, W., Trafford, A. W. & Eisner, D. A. (1998). 2,3-Butanedione monoxime (BDM) decreases sarcoplasmic reticulum Ca^{2+} content by stimulating Ca^{2+} release in isolated rat ventricular myocytes. *Pflügers Archiv* **436**, 776–781.

Allen, T. J., Mikala, G., Wu, X. & Dolphin, A. C. (1998). Effects of 2,3-butanedione monoxime (BDM) on calcium channels expressed in *Xenopus* oocytes. *Journal of Physiology* **508**, 1–14.

Armstrong, C. M. (1992). Voltage-dependent ion channels and their gating. *Physiological Reviews* **72** (4 Suppl.), S5–13.

Armstrong, C. M. & Bezanilla, F. (1977). Inactivation of the sodium channel. II. Gating current experiments. *Journal of General Physiology* **70**, 567–590.

Ashmore, J. F. (1989). Transducer motor coupling in cochlear outer hair cells. In *Cochlear Models: Structure, Function and Models*, ed. Wilson, J. P. & Kemp, D. T., pp. 107–114. Plenum Publishing Corp., New York.

Chertoff, M. E. & Brownell, W. E. (1994). Characterization of cochlear outer hair cell turgor. *American Journal of Physiology* **266**, C467–479.

Coling, D. E., Bartolami, S., Rhee, D. & Neelands, T. (1998). Inhibition of calcium-dependent motility of cochlear outer hair cells by the protein kinase inhibitor, ML-9. *Hearing Research* **115**, 175–183.

Coulombe, A., Lefevre, I. A., Deroubaix, E., Thuringer, D. & Coraboeuf, E. (1990). Effect of 2,3-butanedione 2-monoxime on slow inward and transient outward currents in rat ventricular myocytes. *Journal of Molecular and Cellular Cardiology* **22**, 921–932.

Dieler, R., Shehata-Dieler, W. E. & Brownell, W. E. (1991). Concomitant salicylate-induced alterations of outer hair cell subsurface cisternae and electromotility. *Journal of Neurocytology* **20**, 637–653.

Dulon, D., Zajic, G. & Schacht, J. (1990). Increasing intracellular free calcium induces circumferential contractions in isolated cochlear outer hair cells. *Journal of Neuroscience* **10**, 1388–1397.

Eisfeld, J., Mikala, G., Varadi, G., Schwartz, A. & Klockner, U. (1997). Inhibition of cloned human L-type cardiac calcium channels by 2,3-butanedione monoxime does not require PKA-dependent phosphorylation sites. *Biochemical and Biophysical Research Communications* **230**, 489–492.

Ferreira, G., Artigas, P., Pizarro, G. & Brum, G. (1997). Butanedione monoxime promotes voltage-dependent inactivation of L-type calcium channels in heart. Effects on gating currents. *Journal of Molecular and Cellular Cardiology* **29**, 777–787.

Frolenkov, G. I., Atzori, M., Kalinec, F., Mammano, F. & Kachar, B. (1998). The membrane-based mechanism of cell motility in cochlear outer hair cells. *Molecular Biology of the Cell* **9**, 1961–1968.

Frolenkov, G. I., Kalinec, F., Tavartkiladze, G. A. & Kachar, B. (1997). Cochlear outer hair cell bending in an external electric field. *Biophysical Journal* **73**, 1665–1672.

Frolenkov, G. I., Mammano, F., Belyantseva, I. A., Coling, D. & Kachar, B. (2000). Two distinct Ca^{2+}-dependent signaling pathways regulate the motor output of cochlear outer hair cells. *Journal of Neuroscience* **20**, 5940–5948.

Gale, J. E. & Ashmore, J. F. (1994). Charge displacement induced by rapid stretch in the basolateral membrane of the guinea-pig outer hair cell. *Proceedings of the Royal Society* B **255**, 243–249.

Gale, J. E. & Ashmore, J. F. (1997). An intrinsic frequency limit to the cochlear amplifier. *Nature* **389**, 63–66.

Géléoc, G. S., Casalotti, S. O., Forge, A. & Ashmore, J. F. (1999). A sugar transporter as a candidate for the outer hair cell motor. *Nature Neuroscience* **2**, 713–719.

Green, A. L. & Saville, B. (1956). The reaction of oxime with isopropyl methylphosphonofluoridate (sarin). *Journal of the Chemical Society* **756**, 3887–3892.

Haystead, T. A., Sim, A. T., Carling, D., Honnor, R. C., Tsukitani, Y., Cohen, P. & Hardie, D. G. (1989). Effects of the tumour promoter okadaic acid on intracellular protein phosphorylation and metabolism. *Nature* **337**, 78–81.

Hidaka, H., Sasaki, Y., Tanaka, T., Endo, T., Ohno, S., Fujii, Y., & Nagata, T. (1981). N-(6-Aminohexyl)-5-chloro-1-naphthalene-sulfonamide, a calmodulin antagonist, inhibits cell proliferation. *Proceedings of the National Academy of Sciences of the USA* **78**, 4354–4357.

Holley, M. C., Kalinec, F. & Kachar, B. (1992). Structure of the cortical cytoskeleton in mammalian outer hair cells. *Journal of Cell Science* **102**, 569–580.

Huang, G. & Santos-Sacchi, J. (1993). Mapping the distribution of the outer hair cell motility voltage sensor by electrical amputation. *Biophysical Journal* **65**, 2228–2236.

Ikeda, K. & Takasaka, T. (1993). Confocal laser microscopical images of calcium distribution and intracellular organelles in the outer hair cell isolated from the guinea pig cochlea. *Hearing Research* **66**, 169–176.

Itoh, H. & Hidaka, H. (1984). Direct interaction of calmodulin antagonists with Ca^{2+}/calmodulin-dependent cyclic nucleotide phosphodiesterase. *Journal of Biochemistry* **96**, 1721–1726.

Iwasa, K. H. (1993). Effect of stress on the membrane capacitance of the auditory outer hair cell. *Biophysical Journal* **65**, 492–498.

Johnson, J. D. & Wittenauer, L. A. (1983). A fluorescent calmodulin that reports the binding of hydrophobic inhibitory ligands. *Biochemical Journal* **211**, 473–479.

Kakehata, S. & Santos-Sacchi, J. (1995). Membrane tension directly shifts voltage dependence of outer hair cell motility and associated gating charge. *Biophysical Journal* **68**, 2190–2197.

Kakehata, S. & Santos-Sacchi, J. (1996). Effects of salicylate and lanthanides on outer hair cell motility and associated gating charge. *Journal of Neuroscience* **16**, 4881–4889.

Kalinec, F., Holley, M. C., Iwasa, K. H., Lim, D. J. & Kachar, B. (1992). A membrane-based force generation mechanism in auditory sensory cells. *Proceedings of the National Academy of Sciences of the USA* **89**, 8671–8675.

Kalinec, F. & Kachar, B. (1993). Inhibition of outer hair cell electromotility by sulfhydryl specific reagents. *Neuroscience Letters* **157**, 231–234.

Lee, K., Rowe, I. C. & Ashford, M. L. (1995). Characterization of an ATP-modulated large conductance Ca^{2+}-activated K^+ channel present in rat cortical neurones. *Journal of Physiology* **488**, 319–337.

McKillop, D. F., Fortune, N. S., Ranatunga, K. W. & Geeves, M. A. (1994). The influence of 2,3-butanedione 2-monoxime (BDM) on the interaction between actin and myosin in solution and in skinned muscle fibres. *Journal of Muscle Research and Cell Motility* **15**, 309–318.

Perreault, C. L., Mulieri, L. A., Alpert, N. R., Ransil, B. J., Allen, P. D. & Morgan, J. P. (1992). Cellular basis of negative inotropic effect of 2,3-butanedione monoxime in human myocardium. *American Journal of Physiology* **263**, H503–510.

Puschner, B. & Schacht, J. (1997). Calmodulin-dependent protein kinases mediate calcium-induced slow motility of mammalian outer hair cells. *Hearing Research* **110**, 251–258.

Santos-Sacchi, J. (1991). Reversible inhibition of voltage-dependent outer hair cell motility and capacitance. *Journal of Neuroscience* **11**, 3096–3110.

Santos-Sacchi, J. & Huang, G. (1998). Temperature dependence of outer hair cell nonlinear capacitance. *Hearing Research* **116**, 99–106.

Santos-Sacchi, J., Kakehata, S. & Takahashi, S. (1998). Effects of membrane potential on the voltage dependence of motility-related charge in outer hair cells of the guinea-pig. *Journal of Physiology* **510**, 225–235.

Schulte, B. A. (1993). Immunohistochemical localization of intracellular Ca^{2+}-ATPase in outer hair cells, neurons and fibrocytes in the adult and developing inner ear. *Hearing Research* **65**, 262–273.

Shehata, W. E., Brownell, W. E. & Dieler, R. (1991). Effects of salicylate on shape, electromotility and membrane characteristics of isolated outer hair cells from guinea pig cochlea. *Acta Otolaryngologica* **111**, 707–718.

Smith, P. A., Williams, B. A. & Ashcroft, F. M. (1994). Block of ATP-sensitive K^+ channels in isolated mouse pancreatic beta-cells by 2,3-butanedione monoxime. *British Journal of Pharmacology* **112**, 143–149.

Stypulkowski, P. H. (1990). Mechanisms of salicylate ototoxicity. *Hearing Research* **46**, 113–145.

Tolomeo, J. A., Steele, C. R. & Holley, M. C. (1996). Mechanical properties of the lateral cortex of mammalian auditory outer hair cells. *Biophysical Journal* **71**, 421–429.

Tripathy, A., Xu, L., Pasek, D. A. & Meissner, G. (1999). Effects of 2,3-butanedione 2-monoxime on Ca^{2+} release channels (ryanodine receptors) of cardiac and skeletal muscle. *Journal of Membrane Biology* **169**, 189–198.

Tunstall, M. J., Gale, J. E. & Ashmore, J. F. (1995). Action of salicylate on membrane capacitance of outer hair cells from the guinea-pig cochlea. *Journal of Physiology* **485**, 739–752.

Waurick, R., Knapp, J., Van Aken, H., Bokník, P., Neumann, J., & Schmitz, W. (1999). Effect of 2,3-butanedione monoxime on force of contraction and protein phosphorylation in bovine smooth muscle. *Naunyn-Schmiedeberg's Archives of Pharmacology* **359**, 484–492.

Wilson, I. R. & Ginsburg, S. (1955). A powerful reactivator of alkyl-phosphate inhibited acetylcholinesterase. *Biochemical and Biophysical Research Communications* **18**, 168–170.

Wu, M. & Santos-Sacchi, J. (1998). Effects of lipophilic ions on outer hair cell membrane capacitance and motility. *Journal of Membrane Biology* **166**, 111–118.

Ye, J. H. & McArdle, J. J. (1995). Excitatory amino acid induced currents of isolated murine hypothalamic neurons and their suppression by 2,3-butanedione monoxime. *Neuropharmacology* **34**, 1259–1272.

Zheng, J., Shen, W., He, D. Z. Z., Long, K. B., Madison, L. D. & Dallos, P. (2000). Prestin is the motor protein of cochlear outer hair cells. *Nature* **405**, 149–155.

Acknowledgements

This work was supported by the National Institutes on Deafness and other Communication Disorders (Intramural research project Z01 DC 00002-11) and in part by grants from Istituto Nazionale di Fisisca della Materia (Progetto di Ricerca Avanzata *CADY*) and Ministero della Ricerca Scientifica to F.M. We thank Kuni Iwasa and Richard Chadwick for critical comments and helpful discussions.

Corresponding author

B. Kachar: NIDCD–NIH, Section on Structural Cell Biology, 9000 Rockville Pike, Bldg 36/5D15, Bethesda, MD 20892-4163, USA.

Email: kacharb@nidcd.nih.gov